In Vitro Growth of Alzheimer's Disease β-Amyloid Plaques Displays First-Order Kinetics[†]

William P. Esler,[‡] Evelyn R. Stimson,[‡] Joseph R. Ghilardi,[§] Harry V. Vinters,[∥] Jonathan P. Lee,[⊥] Patrick W. Mantyh,[§] and John E. Maggio*,[‡]

Department of Biological Chemistry and Molecular Pharmacology, Harvard Medical School, 240 Longwood Avenue, Boston, Massachusetts 02115, Molecular Neurobiology Laboratory, Veteran's Administration Medical Center and Department of Psychiatry, University of Minnesota, Minneapolis, Minnesota 55417, Department of Pathology & Laboratory Medicine and Brain Research Institute, University of California Los Angeles Medical Center, Los Angeles, California 90024, and Department of Chemistry, Boston University, Boston, Massachusetts 02215

Received July 21, 1995; Revised Manuscript Received October 2, 1995[⊗]

ABSTRACT: A salient pathological feature of Alzheimer's disease (AD) is the presence of amyloid plaques in the brains of affected patients. The plaques are predominantly composed of human β-amyloid peptide (Aβ). Although the aggregation of synthetic Aβ has been extensively studied, the mechanism of AD plaque growth is poorly understood. In order to address this question, we used an *in vitro* model of plaque growth to determine if assembly or aggregation of Aβ is required for deposition. Labeled Aβ at physiological concentrations readily deposited onto both neuritic and diffuse plaques and cerebrovascular amyloid in unfixed AD brain tissue, whereas essentially no deposition was detected in tissue without preformed amyloid. Using this *in vitro* model of plaque growth, the kinetics of Aβ deposition onto plaques was examined in two independent but complementary systems. Intact sections of unfixed AD brain cortex (analyzed by autoradiographic densitometry) allowed definitive morphological analysis of the site of deposition, while homogenates of the same tissue (analyzed by radioisotope counting) allowed precise quantitation of deposition over a wide range of conditions. Essentially identical results were obtained for both systems. Growth of preexisting tissue plaques by deposition of Aβ was found to follow first-order dependence on Aβ concentration and exhibited a pH optimum of 7. In sharp contrast, Aβ aggregation in the absence of template follows higher order kinetics and shows a pH optimum of 5. On the basis of criteria of kinetic order, pH dependence, and structure−activity relationships, we conclude that aggregation of Aβ (template-independent initial nidus formation) and deposition of Aβ (template-dependent subsequent plaque growth) are fundamentally distinct biochemical processes. The process of plaque growth and maturation by Aβ deposition may be an important target for therapeutic intervention to block the progression of AD.

Alzheimer's disease (AD)[1] is the third leading cause of death in the elderly of the developed world after cardiovascular disease and cancer (Hardy & Allsop, 1991). This widespread progressive dementia is characterized by the presence of proteinaceous deposits in the brain described as amyloid on the basis of tinctorial properties. These lesions are composed largely of a hydrophobic 39−43 amino acid peptide (Glenner & Wong, 1984) called β-amyloid peptide (Aβ). The extracellular amyloid is deposited at both neuropil and vascular sites and is widely believed to be involved in the progressive neurodegeneration of the disease (Selkoe, 1991, 1994; Mattson et al., 1992; Pike et al., 1991b, 1993, 1995; Kowall et al., 1992). Aβ is encoded by a gene for a much larger protein termed the β-amyloid precursor protein (βPP) (Goldgaber et al., 1987; Kang et al., 1987; Tanzi et al., 1987). Aβ is constitutively produced by cells and present at similar levels ($\approx 10^{-9}$ M) in normal and AD cerebrospinal fluid (CSF) (Haass et al., 1992; Busciglio et al., 1993; Seubert et al., 1992; Shoji et al., 1992; van Gool et al., 1994). Although Aβ(1−40) is the major form of Aβ in CSF (van Gool et al., 1994), recent work suggests that AD amyloid deposits are heterogeneous and contain Aβ(1−42) (Younkin, 1995; Suzuki et al., 1994; Roher et al., 1993; Yang et al., 1994). Evidence that Aβ plays a causative role in AD pathology has come from several observations (Selkoe, 1991, 1994). Aβ is toxic to neurons in culture under some conditions (Pike et al., 1991a,b, 1993, 1995; Roher et al., 1991; Fraser et al., 1994; Busciglio et al., 1992; Yankner et al., 1990; Fukuchi et al., 1993), and plaque formation in the brains of transgenic animals overexpressing the human Aβ peptide also leads to neuronal toxicity (Games et al., 1995). The pathogenic role of Aβ in AD (Cummings et al., 1995; Terry et al., 1991) has also been buttressed by the discovery of several mutations in Aβ or βPP tightly linked to inherited forms of the disease (Mullan & Crawford, 1993).

[†] This research was supported by grants from the National Institutes of Health (AG-12853, AG-10123, AG-12435, AG-11852) and the American Health Assistance Foundation (94071).

* Corresponding author. Tel.: (617) 432-0757. FAX: (617) 432-3833.

[‡] Harvard Medical School.

[§] University of Minnesota.

[∥] University of California.

[⊥] Boston University.

[⊗] Abstract published in *Advance ACS Abstracts,* December 15, 1995.

[1] Abbreviations: Aβ, β-amyloid peptide; AD, Alzheimer's disease; βPP, β-amyloid precursor protein; BSA, bovine serum albumin; CERAD, Consortium to Establish a Registry of Alzheimer's Disease; Ci/mmol; Curies per millimole; CSF, cerebrospinal fluid; DMSO, dimethyl sulfoxide; HFIP, 1,1,1,3,3,3-hexafluoro-2-propanol; ^{125}I-Aβ, ^{125}I-iodotyrosine^{10}-human Aβ(1−40)-OH; RP-HPLC, reverse-phase high-performance liquid chromatography; Tris, Tris(hydroxymethyl)-aminomethane.

0006-2960/96/0435-749$12.00/0

Table 1: Neuropathological Analysis of Cases Used in this Study[a,b]

case	AD1	AD2	AD3	AD4	CON1	CON2
age/sex	85/F	89/M	70/F	63/M	78/M	78/M
PMI (h)	4	3	12	6	11	14
AD	yes	yes	yes	yes	no	no
SP	++	+++	+++	++	−	−
CAA	++	−	+++	++	−	−
NFT	+++	−	+++	++	BrStm, Cb Hc (rare)	−
GVD	+++	+++	+++	+	+	−
other	brain atrophy	severe cortical atrophy	brain atrophy	cortical atrophy	PSP	none

[a] Neuropathological findings were graded semiquantitatively as absent (−), mild/slight (+), moderate (++), or severe (+++). Diagnosis was in accordance with the criteria of CERAD (Gearing et al., 1995) and of Khachaturian (1985). [b] Abbreviations: BrStm, brain stem; CAA, cerebral amyloid angiopathy; Cb, cerebellum; F, female; GVD, granulovacuolar degeneration; Hc, hippocampus; M, male; NFT, neurofibrillary tangles; PMI, time interval from death to tissue collection; PSP, progressive supranuclear palsy; SP, senile plaque.

Many risk factors have been proposed for AD. How each of these factors contributes to the disease is unknown, but it has been suggested that a common mechanism is the generation of neurotoxic Aβ aggregates in the brain (Hardy & Allsop, 1991; Joachim & Selkoe, 1992). The amyloid peptide has been shown to self-assemble into filamentous aggregates (Kirschner et al., 1987; Halverson et al., 1990; Hilbich et al., 1991; Burdick et al., 1992; Castaño et al., 1986), and this process has been linked to the toxicity of Aβ observed in cultured neurons (Pike et al., 1991a,b, 1993, 1995; Mattson et al., 1992; Yankner et al., 1990). As a consequence, much of the work on Aβ has focused on understanding the aggregation properties of the peptide. Several factors that affect its aggregation (including apolipoprotein E isoforms, α_1-antichymotrypsin, and certain metals) have been identified and are the focus of biochemical or genetic studies (Mantyh et al., 1993; Bush et al., 1994a,b; Esler et al., 1996; Evans et al., 1995; Ma et al., 1994; Sanan et al., 1994; Wisniewski & Frangione, 1992; Wisniewski et al., 1995; Fraser et al., 1992a).

Previously, we reported an *in vitro* assay for plaque growth using deposition of radiolabeled Aβ onto preexisting plaques in sections or homogenates of unfixed AD cortex (Mantyh et al., 1991; Maggio et al., 1992), an experimental system of significant physiological relevance. Recent evidence suggests that a structural transition (Lee et al., 1995) may be a necessary step in the conversion of solution Aβ into amyloid plaque. Thus plaque growth may involve an aggregation-independent structural transition. Since dementia has been observed to be correlated with the density of mature AD plaques (Selkoe, 1994; Cummings et al., 1995), a detailed biochemical understanding of plaque growth could help to identify a potential drug target for therapeutic intervention. In this study, we have examined the kinetics of Aβ deposition as a function of pH and Aβ concentration in two types of unfixed tissue preparations to address whether an assembly[2] or aggregation step is required for an Aβ molecule to deposit onto a preexisting plaque (β-sheet) template.

METHODS AND MATERIALS

Synthetic Peptides. Aβ(1−40) synthesized by fluorenylmethoxycarbonyl chemistry was purchased (QCB, Inc., Hopkinton, MA) and stored either lyophilized or as stock solutions (10^{-3} M) in 75% dimethyl sulfoxide (DMSO)/25% hexafluoro-2-propanol (HFIP) at −20 °C to reduce Aβ aggregation during storage. Under these conditions, no evidence of oxidation, degradation, or aggregation was observed over months of storage. To insure that no aggregates were present in the assays, stock solutions were routinely centrifuged (15 000*g* x 10 min) to remove particulates. Peptides were characterized by reverse-phase HPLC (RP-HPLC), laser desorption mass spectrometry, and amino acid analysis (Benson et al., 1981) and gave satisfactory results in all cases. Aβ(1−40), the major form of Aβ found in CSF (Seubert et al., 1992), was used in all experiments. Concentrations of Aβ solutions were determined by amino acid analysis. Four distinct synthetic batches of Aβ and more than 10 distinct synthetic batches of ^{125}I-Aβ were used in the present study; no batch to batch variation was detected.

Radioiodination. Peptides for radioiodination were purified to near homogeneity (>98%) by RP-HPLC with a gradient of acetonitrile in 0.01 M trifluoroacetic acid and a C_{18} column. Radioiodination was by the method of Maggio et al. (1992). Briefly, Aβ(1−40) was radiolabeled at the tyrosine residue at position 10 by oxidative iodination using Na^{125}I and chloramine T. Peptide and unincorporated iodine were separated using reverse-phase adsorption. The oxidized methionine residue at position 35 was reduced from the sulfoxide to the native thioether form using 2-mercaptoethanol. The radioiodinated Aβ(1−40) peptide was purified to a specific activity of about 2000 Ci/mmol (10^9 dpm/μg, one ^{125}I per molecule) by RP-HPLC. The labeled peptides were stored at −20 °C in the eluted HPLC mobile phase. 2-Mercaptoethanol (0.5%) was added to all stock tracer solutions to prevent oxidation during storage.

Tissue. Brain tissue was obtained from AD patients, normal patients, and patients with non-AD degenerative conditions (e.g., progressive supranuclear palsy) at <15 h postmortem, frozen on dry ice after collection, and stored below −20 °C until use. The cases used in the present study are summarized in Table 1. Diagnosis of AD was based on the criteria of the Consortium to Establish a Registry of Alzheimer's Disease (CERAD) (Gearing et al., 1995) and those of Khachaturian (1985), with identification of plaques and plaque subtypes by both classical silver (modified Bielschowsky) stains and anti-Aβ immunohistochemistry (Vinters et al., 1990). For homogenate binding studies, tissue homogenates were prepared by a modification of the method of Too and Hanley (1988). Briefly, tissue was homogenized (Polytron) in 5 volumes of cold 50 mM Tris HCl, pH 7.5, containing 10% (w/v) sucrose and protease inhibitors (0.01% bacitracin, 0.002% soybean trypsin inhibitor, 0.002% chicken-egg trypsin inhibitor, and 1 mM benzamidine). The homo-

[2] The terms "aggregation" and "assembly" are used in accordance with definitions set forth by the ACS Symposia Series on aggregation and denaturation (Hermansson, 1979).

genates were centrifuged at 10 000*g* for 20 min. The resulting pellets were resuspended in 10 volumes of cold 50 mM Tris HCl, pH 7.5, and centrifuged at 40 000*g* for 15 min. After the latter wash procedure was repeated, the pellets were resuspended in 1 volume of Tris HCl buffer. The homogenate was aliquoted to microcentrifuge tubes and was centrifuged at 15 000*g* for 15 min. The supernatants were discarded and the pellets were frozen on dry ice and stored at −20 °C until use (no longer than 4 months). Protein concentrations in the membrane homogenates were determined by dye binding assays (Bio-Rad) using bovine serum albumin (BSA) as standard.

To determine the amount of amyloid binding component retained throughout the homogenization procedure, ^{125}I-Aβ (approximately 10^5 cpm/g of tissue) and $MnCl_2$ (10 mM) were added during some tissue preparations after the initial homogenization, and the homogenate was incubated with tracer for 2 h prior to the first centrifugation. The procedure was followed as outlined above except that aliquots of the supernatants were reserved for γ-counting. This modification allowed for tracking the Aβ binding component (plaque) and quantification of the amount present in the final pellets. Significant enrichment of the Aβ binding component was observed through the above procedure.

Homogenate Binding. Brain membrane homogenate binding was performed in a manner similar to that described (Mantyh et al., 1991; Maggio et al., 1992). Membranes were resuspended and preincubated for 30 min in 50 mM Tris HCl, pH 7.5, containing BSA (1 mg/mL), 0.004% bacitracin, 0.0002% chymostatin, 0.0002% leupeptin, 0.3% DMSO, and 10 mM $MnCl_2$. ^{125}I-Aβ or mixtures of ^{125}I-Aβ and unlabeled Aβ were dissolved in 50 mM Tris HCl, pH 7.5 (except where noted), containing BSA, protease inhibitors, and $MnCl_2$ as above and aliquoted to flexible vinyl 96-well assay plates (Dynatech Laboratories 001-010-2401). The membrane suspension was mixed with the radioligand solution at time zero to yield final total Aβ concentrations of 10^{-11} to 10^{-7} M and membrane levels of 0.63−10 mg of equivalent weight of tissue per well in a final volume of 170 μL. After the desired incubation time (0.5−24 h), samples were centrifuged at 595*g* for 6 min (Sorvall H-1000B rotor equipped with Sorvall Micro-Plate Carriers). Each pellet was washed twice with 50 mM buffer by resuspension and centrifugation. Wells containing washed pellets were capped and separated for γ-counting. Control experiments were performed using age-matched plaque-free (non-AD) human cortex, AD or non-AD cerebellum (unlike cortex, cerebellum is spared in AD), or no tissue to determine background binding. In all cases background in the absence of tissue was less than 5% of the observed deposition onto AD cortex. Deposition rates were determined from the slopes of lines fitted to points of deposition versus time (Figures 5 and 6).

Deposition onto Plaques in Brain Tissue Sections. For autoradiography, serial sections (15 μm) of frozen unfixed human brain tissue were cut on a cryostat microtome and mounted onto gelatin-coated microscope slides. Deposition assays using sections of AD cortex were performed as described by Maggio et al. (1992). Briefly, slide-mounted tissue sections were preincubated for 30 min under the conditions described for homogenate binding experiments. They were then incubated for various lengths of time (1−6 h) with various concentrations of labeled Aβ peptide (10^{-11}−10^{-8} M). After the desired incubation period, the sections were thoroughly washed, dried, and placed on film alongside radioiodinated standards. After exposure at 22 °C, the film was developed, fixed, and washed. The density of radioligand bound to tissue amyloid was determined quantitatively using microdensitometry. Sections compared by densitometry within a given experiment were cut from a single tissue block with essentially uniform plaque density throughout. Autoradiograms produced from the ^{125}I-Aβ deposition experiments were placed on a stabilized, uniformly lit fluorescent light box. The autoradiograms were viewed through a high-resolution CCD camera attached to a dissecting microscope. The resulting video image was electronically transferred to the NIH Image program (version 1.41) for analysis.

The grayscale (optical density) values of radioiodinated standards were measured and the data curve-fit was calibrated to correct for the nonlinearity of the film. Calibrated background optical density measurements were recorded and subtracted from all subsequent tissue measurements. Spatial occupation of the labeled amyloid deposits within the field was measured electronically using NIH Image. Results are reported as the product of [optical density] × [area covered by the labeled plaques] in the autoradiograms. Rates of Aβ deposition were calculated as the fitted slopes of [OD] × [area] versus time.

RESULTS

Aβ Deposition onto Plaques in AD Cortical Sections. As previously reported, ^{125}I-Aβ was found to deposit onto tissue amyloid in unfixed AD cortical sections in a specific and nonsaturable manner (Maggio et al., 1992; Mantyh et al., 1991). In all cases, visualization of binding sites for ^{125}I-Aβ by autoradiography showed that Aβ was deposited onto parenchymal amyloid plaques and vascular sites in the AD brain (Figure 1a; Maggio et al., 1992). Classical silver staining and anti-Aβ immunohistochemistry indicated that in the AD cerebral cortex, ^{125}I-Aβ was deposited onto compact, diffuse, and neuritic plaques; in the latter case both the core and halo of essentially every plaque were labeled (Maggio et al., 1992). In contrast to the AD cortex, in which as much as one-third of the affected gray matter area was occupied by plaques competent at binding ^{125}I-Aβ, essentially no such deposits were observed in non-AD cortex (Figure 1b) at all peptide concentrations and times tested (not shown). No significant oxidation or degradation of peptide in solutions exposed to tissue were observed by RP-HPLC.

Deposition onto plaques in sections of unfixed AD cortex was found to be a pH-dependent process with a broad maximum at pH 7 (Figure 2a, solid symbols). There was essentially no deposition below pH 4 or above pH 10. At a pH of 5.5 (used for NMR spectroscopy; Lee et al., 1995), about 70% of the maximum binding activity was retained.

A representative set of autoradiograms of sections incubated with 50 pM ^{125}I-Aβ for different times (Figure 3) demonstrates that the amount of ^{125}I-Aβ bound to the tissue plaques increased with time. Similarly, the amount of ^{125}I-Aβ deposited over a fixed time period increased with ^{125}I-Aβ concentration (Figure 4). When the amount of ^{125}I-Aβ deposited onto plaques in sections was quantified, deposition was found to increase linearly with time and was nonsaturable at or around physiological concentrations. Similar results were observed over all concentrations tested (10−2000 pM). A "lag time" suggestive of a nucleation-dependent process (Jarrett & Lansbury, 1993) was not observed in any case. The rate of deposition increased linearly with increasing concentrations of Aβ (Figures 4 and 5).

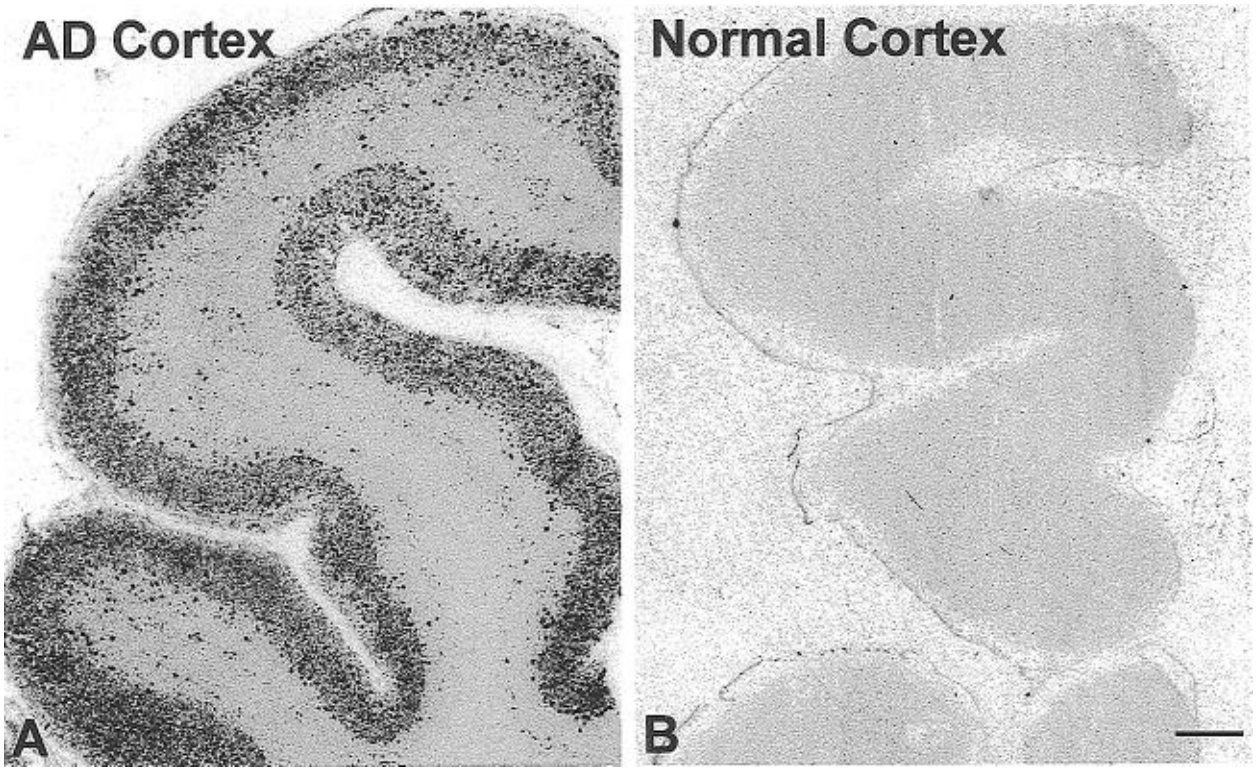

FIGURE 1: Aβ deposition onto unfixed AD or normal human cortex. Slide-mounted sections of AD (A) (case AD4) or control plaque-free non-AD (B) (case CON1) human frontal cortex were incubated in the presence of 100 pM ^{125}I-Aβ for 2 h as described in the text. The sections were washed thoroughly and placed in apposition to X-ray film alongside radioiodinated standards (exposure = 6 days). The prints shown are brightfield autoradiograms of identical exposure. Dark areas represent silver grains overlying areas of ^{125}I-Aβ deposition, which correspond to histochemically identified amyloid present in the tissue. Similar results (not shown) were observed with 10 other AD cases and seven other non-AD cases (Mantyh et al., 1991). Scale bar = 0.163 cm.

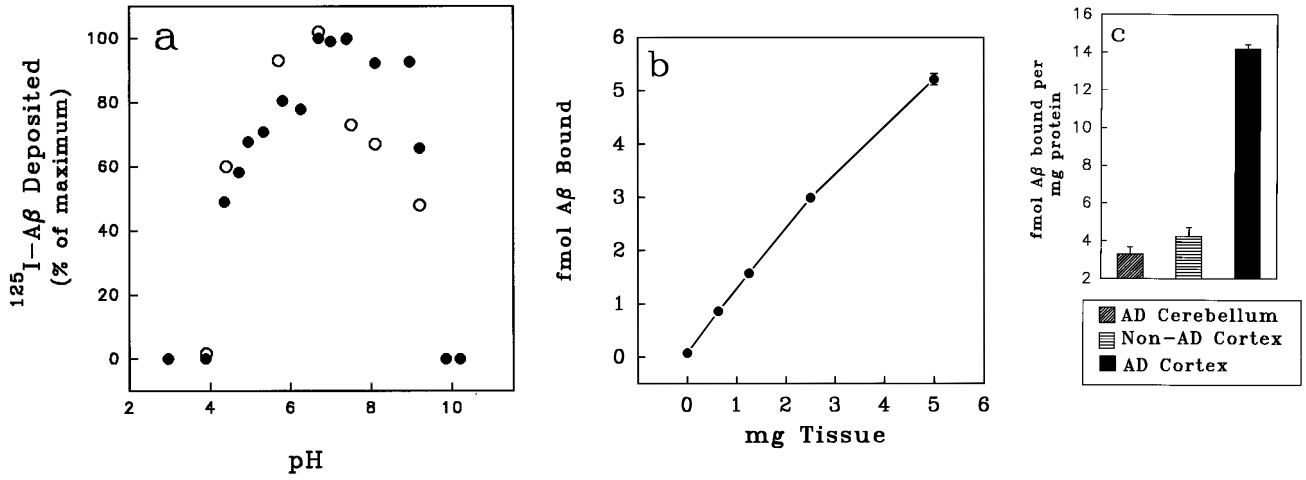

FIGURE 2: Characterization of Aβ deposition assays. (a) pH dependence of ^{125}I-Aβ deposition onto AD cortex. Plaque growth assays were performed on AD cortex sections (solid symbols) and homogenates (open symbols). Slide-mounted AD cortex sections (case AD4) were incubated in a variety of 50 mM buffer systems. The buffers used were sodium acetate (pH 2−5), 2-(*N*-morpholino)ethanesulfonic acid (pH 4−7), Tris HCl (pH 6−10), and 2-(*N*-cyclohexylamino)ethanesulfonic acid (pH 9−12). In all cases, [^{125}I-Aβ] = 100 pM and incubation times were 2 h. Plaque growth assays on AD cortex homogenates (case AD3) were performed in 50 mM Tris HCl or a 50 mM buffer system composed of ethylenediamine and succinic acid to provide better buffering capacity at acidic and alkaline pH values. In all cases, [^{125}I-Aβ] = 45 pM and incubation times were 2 h. Points represent the mean of at least six determinations. (b) Deposition of ^{125}I-Aβ onto different amounts of human AD cortex homogenate (case AD1). Plaque growth assays were performed on 0−5 mg equivalent weight of tissue per sample as described in the text. Error bars represent the SEM of at least six determinations. Error bars that are not visible are smaller than the symbols. (c) Deposition of Aβ onto AD (case AD2) and control (case CON1) brain tissue homogenates. Homogenates of human AD brain tissue (cortex and cerebellum) and age-matched control tissue (cortex) were prepared as described in the text. Plaque growth assays were performed on the homogenates using a 2 h incubation with 65 pM ^{125}I-Aβ. Values were corrected to reflect changes in the concentration of free ^{125}I-Aβ remaining in solution and are reported relative to the total protein content of each tissue membrane homogenate. Error bars represent the SEM of at least five replicates.

Aβ Deposition onto Plaques in AD Cortical Homogenates. In all tissues tested, ^{125}I-Aβ was also found to bind substantially and reproducibly to plaque-rich homogenates (AD cortex) with only low levels of nonspecific adhesion to plaque-free tissues such as age-matched control cortex and AD or control cerebellum (Figure 2c). In addition, the deposition observed was linearly dependent on the amount of tissue homogenate present (Figure 2b). In parallel

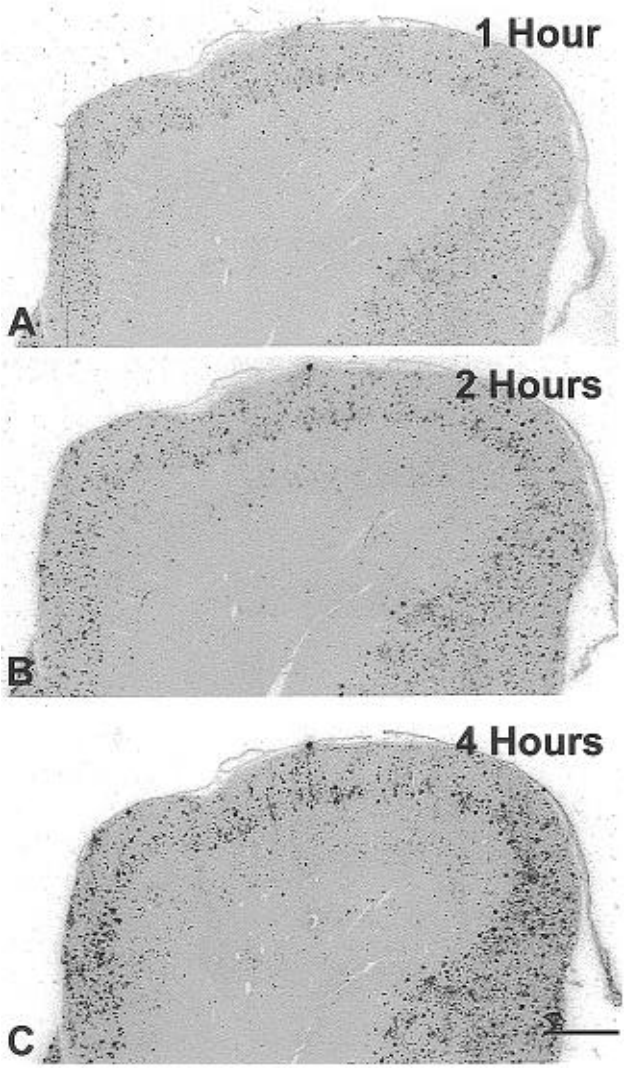

FIGURE 3: ^{125}I-Aβ deposition increases with time. Slide-mounted sections (15 μm) of AD cortex (case AD2) were incubated with 50 pM ^{125}I-Aβ for 1 (A), 2 (B), or 4 (C) h. Sections were then washed, dried, and placed on film as described in the text. Images shown are brightfield autoradiograms of equal exposure (6 days) to illustrate quantitative differences between the intensities. Scale bar = 0.181 cm.

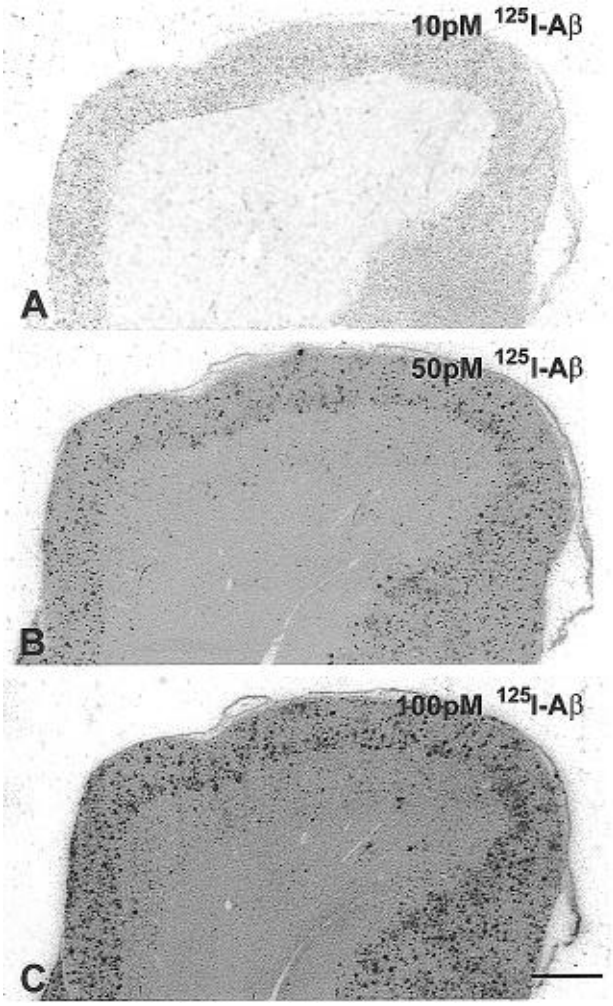

FIGURE 4: ^{125}I-Aβ deposition increases with increases in ^{125}I-Aβ concentration. Slide-mounted sections (15 μm) of AD frontal cortex case (AD2) were incubated for 2 h with ^{125}I-Aβ at 10 pM (A), 50 pM (B), or 100 pM (C) for 2 h. Sections were then examined as described in Figure 3. Scale bar = 0.181 cm.

incubations without tissue, no significant sedimentation of Aβ was observed over a period of at least 24 h (not shown). ^{125}I-Aβ deposition onto plaques in homogenates displayed a similar pH profile (Figure 2a) and similar time courses (Figures 5 and 6) to those found for deposition onto plaques in tissue sections, indicating that the processes of deposition in both preparations are biochemically similar.

When the amount of ^{125}I-Aβ deposited was quantified in tissue homogenates (Figure 6), deposition increased with time and was nonsaturable at or around physiological concentrations. As with tissue sections, deposition onto plaques in homogenates was found to occur at increasing rates with increasing concentrations of Aβ. *In vitro* growth of plaques at physiological Aβ concentrations (on the order of 10^{-10} M) followed linear time dependence for at least 10 h. At much higher concentrations ($>10^{-8}$ M) and longer incubation times (>10 h) rates slowed but retained first order dependence on Aβ concentration (not shown). At concentrations significantly higher still ($>10^{-6}$ M), which are rarely if ever observed physiologically, deposition of Aβ onto homogenates of AD cortex approached zero order with respect to Aβ concentration (not shown). Consistent with results in tissue sections, a "lag time" suggestive of a nucleation-dependent process was never observed over this range of time and concentration in tissue homogenates.

In Vitro Plaque Growth Follows First-Order Kinetics. For each of the Aβ concentrations tested, a rate of deposition was determined from the slope of a line fitted to points of deposition versus time (Figures 5 and 6). Rates for the deposition of Aβ at various concentrations were calculated using mixtures of labeled and unlabeled amyloid peptide in various ratios. When the (initial) rate of deposition was calculated and plotted versus total Aβ concentration, first-order dependence was observed in binding experiments with both homogenates (Figure 7b) and sections (Figure 7a) over the entire range of concentrations tested (10^{-11} to 10^{-7} M and 10^{-11} to (2×10^{-9}) M, respectively). These results further underline the biochemical similarities between the two methods. In all cases, equimolar Aβ solutions containing labeled peptide (alone) or mixtures of labeled and unlabeled peptide (in various proportions) resulted in indistinguishable rates of deposition (Figure 7b). Consistent with previous work from a number of laboratories (Burdick et al., 1992; Esler et al., 1996; Evans et al., 1995; Maggio et al., 1992, 1995), ^{125}I-Aβ was found to accurately track unlabeled Aβ throughout all experiments.

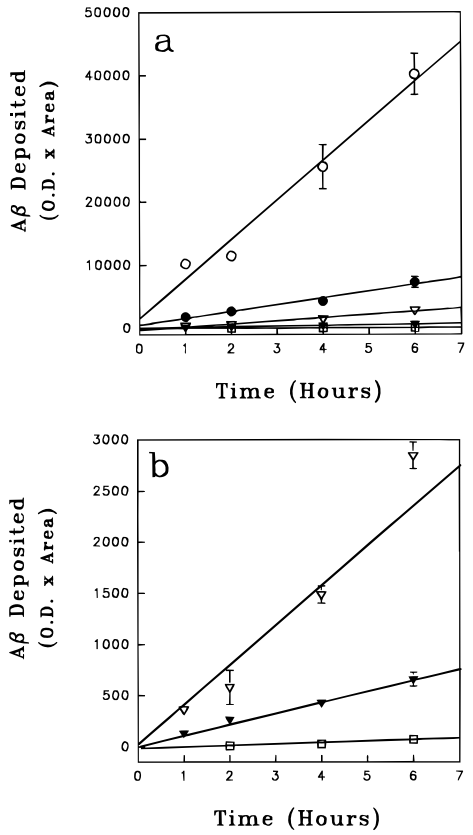

FIGURE 5: Time course of ^{125}I-Aβ deposition onto AD cortex sections from analysis of data such as that shown in Figures 3 and 4. [^{125}I-Aβ] of 2000 (○), 500 (●), 100 (▽), 50 (▼), and 10 pM (□) were used in plaque growth experiments over times of 1−6 h. Error bars represent the SEM of at least three replicates. (a) All of the data (10 pM to 2 nM) are shown. Solid lines represent the initial rate. (b) Vertical expansion of (a) showing the lower ^{125}I-Aβ concentrations (10−100 pM). Data from case AD2.

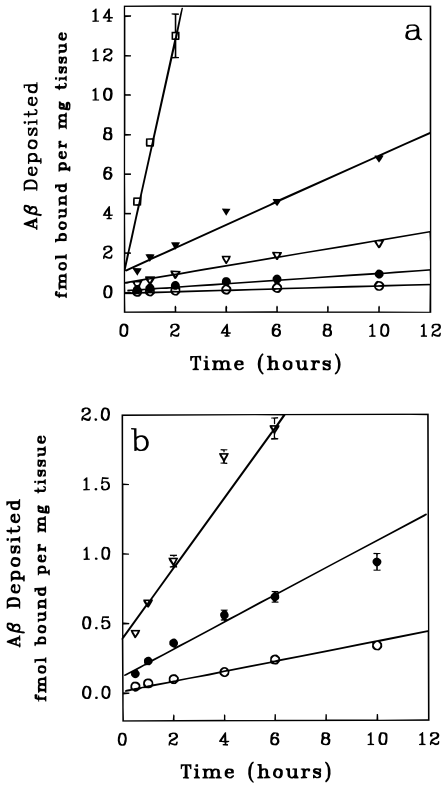

FIGURE 6: Time course of ^{125}I-Aβ deposition onto AD cortex homogenates (case AD1). ^{125}I-Aβ at 11 (○), 33 (●), 100 (▽), 300 (▼), and 1000 pM (□) were used in plaque growth experiments over times of 0.5−10 h. Error bars represent the SEM of 6 to 12 replicates. Error bars that are not visible are smaller than the symbols. (a) All of the data (11−1000 pM) are shown. Solid lines represent the initial rate. (b) Vertical expansion of (a) showing the lower ^{125}I-Aβ concentrations (11−100 pM). All points (a and b) were corrected to reflect changes in the concentration of free ^{125}I-Aβ during the incubation.

DISCUSSION

Amyloid Plaques Serve as a Template for in Vitro Plaque Growth. Previously, we described an *in vitro* model of Aβ plaque growth using Aβ specifically radiolabeled with ^{125}I at tyrosine 10 (^{125}I-Aβ) (Maggio et al., 1992; Mantyh et al., 1991). This highly specific reagent was found to bind with high affinity to diffuse, compact, and neuritic amyloid plaques in unfixed AD cortex (sections or homogenates) at physiological concentrations in aqueous buffers at or near physiological pH. In the present study, this method has been applied to examine the kinetics and pH dependence of Aβ deposition and plaque growth.

The radiolabeled Aβ tracer used in these experiments has been found to behave indistinguishably from the unlabeled Aβ peptide over a wide range of conditions. ^{125}I-Aβ was found to aggregate, deposit onto tissue, and bind to plastic indistinguishably from unlabeled Aβ (Maggio et al., 1992, 1995; Mantyh et al., 1993; Esler et al., 1996). In addition, the assembly and aggregation properties of the iodinated peptide are identical to those of the unlabeled synthetic peptide tracked by colorimetric peptide assay (Burdick et al., 1992) or optical density at 400 nM (Evans et al., 1995). Iodinated Aβ is also recognized by Aβ-specific antisera R-1280 (Tamaoka et al., 1992) in immunochemical experiments (Esler et al., 1996). Consequently, we conclude that the biochemical properties of Aβ important for aggregation, binding, and template recognition are not significantly affected by the specific incorporation of ^{125}I into the tyrosine residue at position ten.

Binding of ^{125}I-Aβ to tissue was dependent on the presence of amyloid plaques in the tissue. In sections of AD cortex, ^{125}I-Aβ deposited onto both mature neuritic plaques and diffuse plaques. In contrast, ^{125}I-Aβ did not significantly bind to sections of plaque-free cortex (Figure 1). Similar results were observed for tissue homogenates. As shown in Figure 2c, incubation of ^{125}I-Aβ with homogenates of plaque-free age-matched control cortex or cerebellum from AD or age-matched control brain resulted in much less binding than was observed for AD cortex. Consistent with previous work (Mantyh et al., 1991), the amount of ^{125}I-Aβ deposited onto AD tissue increased with plaque density (not shown). Since the templates for Aβ deposition in the present study are preexisting brain amyloid deposits which may contain components other than Aβ (Dyrks et al., 1992; Dudek & Johnson, 1994), the precise identity of the Aβ binding component is not addressed by these experiments (Mantyh et al., 1991).

Aβ Deposition Is pH-Dependent. Deposition of Aβ onto plaques in both homogenates and tissue sections followed a broad pH dependence with a maximum at about pH 7. Deposition was insignificant below pH 4 and above pH 10. Results were similar when a variety of buffers were used (Figure 2a). That the pH dependence was similar for deposition onto plaques in homogenates and sections further argues that the processes involved in each of these systems are similar. In contrast, Aβ aggregation (that is, self-

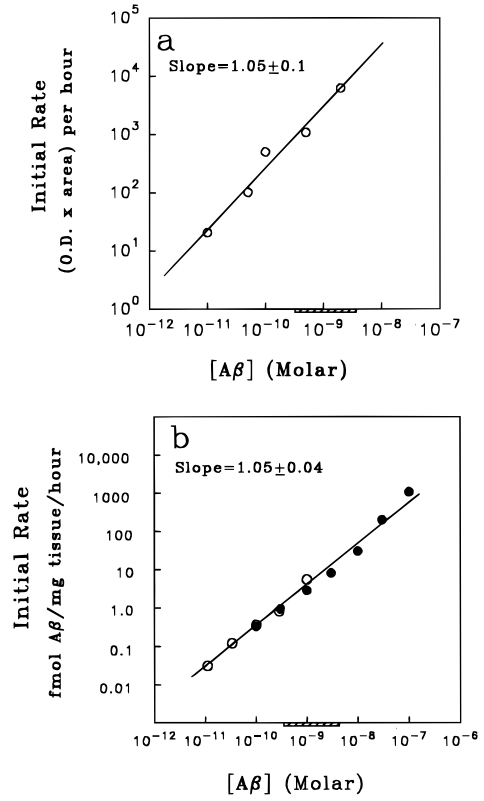

FIGURE 7: Initial rate of Aβ deposition onto AD cortex homogenates or sections versus Aβ concentration. (a) The initial rate of plaque growth was determined for ^{125}I-Aβ deposition onto AD cortex sections using linear regression analysis of data shown in Figures 3−5. The shaded region of the X-axis indicates the physiological range of Aβ concentration in CSF (van Gool et al., 1994). Error bars represent the standard errors on the slopes as determined by regression analysis of the time course data in Figure 5. The slope indicated in the figure was determined from linear regression ($r^2 = 0.98$) of the log−log plot shown. (b) The initial rate of plaque growth was determined for deposition of ^{125}I-Aβ (○) and for the deposition of mixtures of ^{125}I-Aβ and unlabeled Aβ (●) onto AD cortex homogenates using linear regression analysis of time course data in Figure 6. r^2 values ≥ 0.97 were typical for time course data. The point at 10^{-7} M is based on the slope determined by one 0.5 h time point; all others are based on the slope determined from several (≥4) time points. The shaded region of the X-axis indicates the physiological range of Aβ concentration of Aβ in CSF. Error bars represent the standard errors on the slopes as determined by regression analysis of time course data. Error bars that are not visible are smaller than the symbols. The slope indicated in the figure was determined by linear regression ($r^2 = 0.99$) of the log−log plot illustrated. Because the rate at 10^{-7} M was estimated from one time point, it was not included in the regression.

assembly of the peptide in the absence of template) has a significantly lower optimal pH (≈5) near the isoelectric point of the peptide and is negligible above pH 8 (Burdick et al., 1992). The processes of aggregation and deposition have significantly different pH profiles, suggesting that they have different rate-limiting steps.

Aβ Deposition Follows a Linear Time Course. ^{125}I-Aβ deposition experiments were performed over a wide range of concentrations in both tissue homogenates and in tissue sections. In both preparations, the growth of plaques *in vitro* followed a linear time course for at least 10 h over a significant range of Aβ concentrations bracketing physiological values (Figures 5 and 6). Deposition of physiologically relevant concentrations of ^{125}I-Aβ (100 pM) followed a linear time course for at least 48 h (not shown). The observation that the binding is not saturable suggests that the vast majority of sites to which the radioligand binds are not receptors in the usual sense (Maggio et al., 1992). The rate of Aβ deposition in both sections and homogenates increased linearly with increases in Aβ concentration (Figures 5 and 6). Results were identical if the fraction of labeled peptide used was 1%, 10%, or 100% of the total Aβ concentration (not shown); thus experiments with higher total peptide concentrations than could be easily performed with tracer alone could be performed using mixtures of labeled and unlabeled peptide. Over the entire concentration range tested, linear initial time courses were observed and rates increased proportionally with increasing peptide concentrations. Since in all cases tested first-order kinetics were observed, we conclude that Aβ deposition onto plaques is similar over a 10^4-fold range of concentrations around physiological levels.

In contrast to Aβ deposition, aggregation of Aβ (self-assembly in the absence of plaques or other template) into a sedimentable form does not occur under the conditions and at the concentrations ($\leq 10^{-6}$ M) used in the present study, which is a finding consistent with previous reports (Burdick et al., 1992; Jarrett & Lansbury, 1993). At the higher ($\approx 10^{-4}$ M, supersaturated) concentrations where Aβ aggregation does occur, it follows a distinctly nonlinear time course (Come et al., 1993; Evans et al., 1995; Kelly & Lansbury, 1994) with lag times characteristic of rate-limiting nucleation (Jarrett & Lansbury, 1993). This significant difference in the time courses of Aβ deposition onto plaques and Aβ aggregation in template-free systems also argues that the two processes are fundamentally distinct.

Plaque Growth Follows First-Order Kinetics. The progressive senile dementia of AD develops gradually over several years. Since plaque formation and growth are essential pathogenetic processes in the disease (Selkoe, 1994), a detailed biochemical understanding of Aβ deposition may be helpful in understanding its progression. ^{125}I-Aβ deposition onto tissue amyloid in unfixed AD cortex was used in the present study as a model of plaque growth to examine the kinetics of Aβ deposition. When the rates of deposition onto plaques in AD cortex (sections or homogenates) were plotted versus Aβ concentration, a linear response (Figure 7) was observed over the entire concentration range tested (10^{-11} to 10^{-7} M). Hence, the process of plaque growth by deposition of Aβ is first order with respect to Aβ concentration and is nucleation-independent. In sharp contrast, amyloid peptide aggregation shows higher order ($\gg 1$) kinetics (Jarrett et al., 1992, 1993, 1994; Jarrett & Lansbury, 1993; Kelly & Lansbury, 1994). The difference in reaction order between aggregation of Aβ and deposition of Aβ onto AD plaques further confirms that these processes are fundamentally distinct. Fully consistent with the time course data, the kinetic order of Aβ deposition onto plaques establishes that the deposition process is not rate-limited by assembly of peptide oligomer.

The present results suggest that Aβ deposits onto plaques as a monomer. We cannot completely exclude, however, the possibility that the peptide is predominantly in the form of a single stable oligomer (e.g., a dimer; Soreghan et al., 1994) over the entire concentration range (4 orders of magnitude) tested. The ability of Aβ peptides to form dimers and higher order oligomers, however, is critically dependent on the carboxyl-terminal portion of the sequence (Soreghan et al., 1994; Jarrett & Lansbury, 1993). The ability of a truncated (26-mer) form of Aβ lacking this C-terminal region to deposit onto plaques (Lee et al., 1995) with rates similar

to those of the intact 40-mer argues in favor of the monomer as the form of Aβ which supports plaque growth at physiological concentrations.

Aβ Deposition in Sections and Homogenates Is Biochemically Similar. The two tissue preparations (brain homogenates and brain sections) used for deposition experiments in this study provide independent and complementary information. The two preparations are indistinguishable in their dependence of deposition rates upon plaque density, pH, kinetic order, and Aβ concentration. The autoradiographic analysis of Aβ deposition onto plaques in brain sections definitively identifies the site of deposition in intact tissue. Deposition in the homogenate system lacks this histological component but has advantages of simplicity and speed. These parallel methods for examining the same biochemical process provide a powerful combination in assessing factors important in the progression of plaque growth and a means of screening for compounds that may inhibit it.

Aggregation and Deposition of Aβ Are Distinct Processes: Implications for AD. Since the degree of dementia and symptomatology observed in AD is correlated more closely with the density of mature plaques rather than with total amyloid burden (Selkoe, 1994), growth and maturation of plaques are surely important aspects of the disease. *In vitro* plaque growth displays first-order dependence on Aβ concentration. This finding is significant for at least two reasons. Firstly, the first-order kinetics of plaque growth contrast dramatically with the nucleation-dependent higher order kinetic pattern observed for aggregate formation *in vitro* (Come et al., 1993; Evans et al., 1995; Halverson et al., 1990; Jarrett & Lansbury, 1993; Jarrett et al., 1992, 1993, 1994). Assembly of higher order aggregates of Aβ is, thus, not required for *in vitro* plaque growth. Secondly, these results demonstrate that small changes in Aβ concentration result in only small proportional changes in the rate of plaque growth. Small alterations in Aβ concentration would have a much larger effect on the nucleation-dependent process of amyloid peptide aggregation, which would be expected to have a concentration dependence of $[A\beta]^n$, where n is the number of molecules needed to form the nucleating aggregate (Jarrett et al., 1992, 1993). Small increases in Aβ concentration would thus be more likely to affect initial nidus formation (see below) than plaque growth.

Aggregation in solution and deposition of unaggregated Aβ onto a preformed template are two distinct biochemical processes probably involved with two different aspects of AD plaque development (Table 2). Aggregation (in a nucleation-dependent manner) has been shown to be the rate-limiting step in clearing Aβ from solution (Come et al., 1993; Jarrett et al., 1992, 1993; Jarrett & Lansbury, 1993), and the aggregation state of Aβ has been strongly linked to its toxicity against neurons in culture (Pike et al., 1991a,b, 1993, 1995; Mattson et al., 1992). In the present study, deposition of unaggregated Aβ onto tissue was observed only in the presence of a preexisting plaque template. In contrast, in the absence of plaque templates, aggregated Aβ has a greater tendency to adhere to cortical tissue than the unaggregated form (Good & Murphy, 1995). Thus, Aβ aggregation seems likely to be involved in the initial formation of a nidus or template. Once a template is present, plaque growth and maturation could occur via aggregation-independent mechanisms.

Given that Aβ deposition is an essential pathological component in Alzheimer's disease (Selkoe, 1994), the process of plaque growth and maturation may be an important target for therapeutic intervention to block the progression of AD. Unlike Aβ aggregation, which has been reported to occur in response to many factors, deposition of Aβ and consequent plaque growth may occur via a common structural transition (Lee et al., 1995) in Aβ that is independent of the cause of initial nidus formation. Thus a pharmacophore designed to block plaque expansion (by Aβ deposition) and maturation may be more universal than one designed to block aggregation. Over the several-year progression of AD, plaques present in affected patients become associated with other proteins and molecules within them become covalently cross-linked (Dyrks et al., 1992; Dudek & Johnson, 1994); completely dissolving or removing such plaques already present at diagnosis thus faces considerable obstacles. In contrast, inhibiting the further growth of existing plaques, a process which can be modeled under near-physiological concentrations and conditions in assays such as those described here, seems decidedly more feasible.

Table 2: Comparison of Aβ Aggregation[a] and Aβ Deposition onto a Preformed Template

	aggregation	deposition
pH optimum	~5	~7
kinetic order	higher order ($\gg$1)	first order
time dependence	nonlinear with a characteristic lag-time	linear
nucleation dependent	yes	no
template dependent	no	yes
Aβ concentration[b]	$>10^{-6}$ M[c]	10^{-12}–10^{-7} M
relevance to AD	nascent plaque formation (?)	plaque growth

[a] Information for Aβ aggregation taken from Jarrett et al. (1992, 1993, 1994), Jarrett and Lansbury (1993), and Burdick et al. (1992). [b] Concentration of Aβ in human CSF is 2.3 $\pm$ 0.21 nM (van Gool et al., 1994). [c] In the absence of other components. In the presence of other components (such as metal ions), aggregation may occur at lower concentrations (Burdick et al., 1992; Mantyh et al., 1993; Esler et al., 1996).

REFERENCES

Benson, J. R., Louie, P. C., & Bradshaw, R. A. (1981) in *The Peptides, Vol. 4* (Gross, E., Meienhofer, J., Eds.) Vol. 4, pp 217–260, Academic Press, New York.

Burdick, D., Soreghan, B., Kwon, M., Kosmoski, J., Knauer M., Henschen, A., Yates, J., Cotman, C., & Glabe, C. (1992) *J. Biol. Chem. 267*, 546–554.

Busciglio, J., Lorenzo, A., & Yankner, B. A. (1992) *Neurobiol. Aging 13*, 609–612.

Busciglio, J., Gabuzda, D. H., Matsudaira, P., & Yankner, B. A. (1993) *Proc. Natl. Acad. Sci. U.S.A. 90*, 2092–2096.

Bush, A. I., Pettingell, W. H., d. Paradis, M., & Tanzi, R. E. (1994a) *J. Biol. Chem. 269*, 12152–12158.

Bush, A. I., Pettingell, W. H., Multhaup, G., d. Paradis, M., Vonstattel, J.-P., Gusella, J. F., Beyreuther, K., Masters, C. L., & Tanzi, R. E. (1994b) *Science 265*, 1464–1467.

Castaño, E. M., Ghiso, J., Prelli, F., Gorevic, P. D., Migheli, A., & Frangione, B. (1986) *Biochem. Biophys. Res. Commun. 141*, 782–789.

Come, J. H., Fraser, P. E., & Lansbury, P. T., Jr. (1993) *Proc. Natl. Acad. Sci. U.S.A. 90*, 5959–5963.

Cummings, B. J., Pike, C. J., & Cotman, C. W. (1995) *Soc. Neurosci. Abstr. 21*, 1500.

Dudek, S. M., & Johnson, G. U. (1994) *Brain Res. 651*, 129–133.

Dyrks, T., Dyrks, E., Hartmann, T., Masters, C., & Beyreuther, K. (1992) *J. Biol. Chem. 267*, 18210–18217.

Esler, W. P., Stimson, E. R., Jennings, J. M., Ghilardi, J. R., Mantyh, P. W., & Maggio, J. E. (1996) *J. Neurochem.* (in press).

Evans, K. C., Berger, E. P., Cho, C.-G., Weisgraber, K. H., & Lansbury, P. T., Jr. (1995) *Proc. Natl. Acad. Sci. 92*, 763–767.

Fraser, P. E., Nguyen, J. T., Chin, D. T., & Kirschner, D. A. (1992a) *J. Neurochem. 59*, 1531−1540.
Fraser, P. E., Nguyen, J. T., McLachlan, D. R., Abraham, C. R., & Kirschner, D. A. (1992b) *J. Neurochem. 61*, 298−305.
Fraser, P. E., Lévesque, L., & McLachlan, D. R. (1994) *J. Neurochem. 62*, 1227−1230.
Fukuchi, K., Sopher, B., & Martin, G. M. (1993) (1993) *Nature 361*, 122−123.
Games, D., Adams, D., Alessandrini, R., Barbour, R., Bathelette, P., Blackwell, C., Carr, A., Clemens, J., Donaldson, T., Gillepsie, F., Guido, T., Hagopian, S., Johnson-Wood, K., Khan, K., Lee, M., Leibowitz, P., Lieberburg, I., Little, S., Masliah, E., McConlogue, L., Montoya-Zavala, M., Mucke, L., Paganini, L., Penniman, E., Power, M., Schenk, D., Suebert, P., Snyder, B., Soriano, F., Tan, H., Vitale, J., Wadsworth, S., Wolozin, B., & Zhao, J. (1995) *Nature 373*, 523−527.
Gearing, M., Mirra, S. S., Herdreen, J. C., Sumi, S. M., Hansen, L A., & Heyman, A. (1995) *Neurology 45*, 461−466.
Glenner, G. G., & Wong, C. W. (1984) *Biochem. Biophys. Res. Commun. 122*, 1131−1135.
Goldgaber, D., Lerman, J. I., McBride, O. W., Saffioti, U., & Gajdusek, D. C. (1987) *Science 235*, 877−880.
Good, T. A., & Murphy, R. M. (1995) *Biochem. Biophys. Res. Commun. 207*, 209−215.
Haass, C., Schlossmacher, M. G., Hung, A. Y., Vigo-Pelfrey, C., Mellon, A., Ostaszewski, B. L., Lieberburg, I., Koo, E. H., Schenk, D., & Teplow, D. B. (1992) *Nature 359*, 322−325.
Halverson, K., Fraser, P. E., Kirschner, D. A., & Lansbury, P. T., Jr. (1990) *Biochemistry 29*, 2639−2644.
Hardy, J., & Allsop, D. (1991) *Trends Pharmacol. Sci. 12*, 383−388.
Hermansson, A.-M. (1979) *ACS Symp. Ser. 92*, 81−103.
Hilbich, C., Kisters-Woike, B., Reed, J., Masters, C. L., Beyruether, K. (1991) *J. Mol. Biol. 218*, 149−163.
Hyman, B. T., Van Hoesen, G. W., Kroner, L. J., & Damasio, A. R. (1986) *Ann. Neurol. 20*, 472.
Jarrett, J. T., & Lansbury, P. T., Jr. (1992) *Biochemistry 31*, 12345−12354.
Jarrett, J. T., & Lansbury, P. T., Jr. (1993) *Cell 73*, 1055−1058.
Jarrett, J. T., Berger, E. P., & Lansbury, P. T., Jr. (1993) *Biochemistry 32*, 4694−4697.
Jarrett, J. T., Costa, P. R., Griffin, R. G., & Lansbury, P. T., Jr. (1994) *J. Am. Chem. Soc. 116*, 9741−9742.
Joachim, C. L., & Selkoe, D. J. (1992) *Alzheimer Dis. Assoc. Disord. 6*, 7−34.
Kang, J., Lemaire, K. H., Unterbeck, A., Salbaum, J., Masters, C. L., Grsechik, K. H., Multhaup, G., Beyreuther, K., & Müller-Hill, B. (1987) *Nature 325*, 733−736.
Kelly, J. W., & Lansbury, P. T., Jr. (1994) *Amyloid 1*, 186−205.
Khachaturian, Z. S. (1985) *Arch. Neurol. 42*, 1097−1105.
Kirschner, D. A., Inoye, H., Duffy, L. K., Sinclair, A., Lind, M., & Selkoe, D. J. (1987) *Proc. Natl. Acad. Sci. U.S.A. 84*, 6953−6957.
Kowall, N. W., McKee, A. C., Yankner, B. A., & Beal, M. F. (1992) *Neurobiol. Aging 13*, 537−542.
Lee, J. P., Stimson, E. R., Ghilardi, J. R., Mantyh, P. W., Lu, Y.-A., Felix, A. M., Llanos, W., Behbin, A., Cummings, M., Van Criekinge, M., Timms, W., & Maggio, J. E. (1995) *Biochemistry 34*, 5191−5200.
Ma, J., Yee, A., Brewer, H. B., Jr., Das, S., & Potter, H. (1994) *Nature 372*, 92−94.
Maggio, J. E., Stimson, E. R., Ghilardi, J. R., Allen, C. J., Dahl, C. E., Whitcomb, D. C., Vigna, S. R., Vinters, H. V., Labenski, M. E., & Mantyh, P. W. (1992) *Proc. Natl. Acad. Sci. U.S.A. 89*, 5462−5466.
Maggio, J. E., Esler, W. P., Stimson, E. R., Jennings, J. M., Ghilardi, J. R., & Mantyh, P. W. (1995) *Science 267*, 1920−1921.
Mantyh, P. W., Stimson, E. R., Ghilardi, J. R., Allen, C. J., Dahl, C. E., Whitcomb, D. C., Vigna, S. R., Vinters, H. V., Labenski, M. E., & Maggio, J. E. (1991) *Bull. Clin. Neurosci. 56*, 73−85.
Mantyh, P. W., Ghilardi, J. R., Rogers, S., DeMaster, E., Allen, C. J., Stimson, E. R., & Maggio, J. E. (1993) *J. Neurochem. 61*, 1171−1174.
Mattson, M. P., Cheng, B., Davis, D., Bryant, K., Leiberburg, I., & Rydel, R. (1992) *J. Neurosci. 12*, 376−389.
Meienhofer, J., Waki, M., Heimer, E. P., Lambros, R. J., Makofske, R. C., & Chang, C.-D. (1979) *Int. J. Pept. Protein Res. 13*, 35−42.
Mullan, M., & Crawford, F. (1993) *Trends Neurosci. 16*, 398−403.
Pike, C. J., Walencewicz, J., Glabe, C. G., & Cotman, C. W. (1991a) *Eur. J. Pharmacol. 207*, 367−368.
Pike, C. J., Walencewicz, J., Glabe, C. G., & Cotman, C. W. (1991b) *Brain Res. 563*, 311−314.
Pike, C. J., Cummings, B. J., & Cotman, C. W. (1992) *NeuroReport 3*, 769−772.
Pike, C. J., Burdick, D., Walencewicz, J., Glabe, C. G., & Cotman, C. W. (1993) *J. Neurosci. 13*, 1676−1687.
Pike, C. J., Walencewicz-Wasserman, J., Kosmoski, D., Cribbs, H., Glabe, C. G., & Cotman, C. W. (1995) *J. Neurochem. 64*, 253−265.
Roher, A. E., Ball, M. J., Bhave, S. V., & Wakade, A. R. (1991) *Biochem. Biophys. Res. Commun. 174*, 572−579.
Roher, A. E., Lowenson, J. D., Clarke, S., Woods, A. S., Cotter, R. J., Gowing, E., & Ball, M. J. (1993) *Proc. Natl. Acad. Sci. U.S.A. 90*, 10836−10840.
Sanan, D., Weisgraber, K. H., Russell, S. J., Mahley, R. W., Huang, D., Saunders, A., Schmedchel, D., Wisniewski, T., Frangione, B., Roses, A. D., & Strittmatter, W. J. (1994) *J. Clin. Invest. 94*, 860−869.
Selkoe, D. J. (1991) *Neuron 6*, 487−498.
Selkoe, D. J. (1994) *J. Neuropathol. Exp. Neurol. 53*, 438−47.
Seubert, P., Vigo-Pelfry, C., Esch, F., Lee, M., Dovey, H., Davis, D., Sinha, S., Schlossmacher, M., Whaley, J., Swindelhurst, C., McCormack, R., Wolfert, R., Selkoe, D., Lieberburg, I., & Schenck, D. (1992) *Nature 359*, 325−327.
Shoji, M., Golde, T. E., Ghiso, J., Cheung, T. T., Estus, S., Shaffer, L. M., Cai, X. D., McKay, D. M., Titner, R., & Frangione, B. (1992) *Science 258*, 126−129.
Soreghan, B., Kosmoski, J., & Glabe, C. (1994) *J. Biol. Chem. 269*, 28551−54.
Suzuki, N., Cheung, T. T., Cai, X. D., Odaka, A., Otvos, L., Jr., Eckman, C., Golde, T. E., & Younkin, S. G. (1994) *Science 264*, 1336−40.
Talafous, J., Marcinowski, K. J., Klopman, G., & Zagorski, M. G. (1994) *Biochemistry 33*, 7788−7796.
Tanzi, R. E., Gusella, J. F., Watkins, P. C., Bruns, G. A. P., St. George-Hyslop, P., Van Keuren, M. L., Patterson, S. P., Pagan, S., Kurnit, D. M., & Neve, R. L. (1987) *Science 235*, 880−884.
Terry, R. D., Masliah, E., Salmon, D. P., Butters, N., DeTeresa, R., Hill, R., Hansen, L. A., & Katzman, R. (1991) *Ann. Neurol. 30*, 572−580.
Tomaoka, A., Kalaria, R., Lieberburg, I., & Selkoe, D. (1992) *Proc. Natl. Acad. Sci. U.S.A. 89*, 1345−1349.
van Gool, W. A., Kuiper, M. A., Walstra, G. J. M., Wolters, E. Ch., & Bolhuis, P. A. (1994) *Ann. Neurol. 37*, 277−279.
Vinters, H. V., Secor, D. L., Pardridge, W. M., & Gray, F. (1990) *Ann. Neurol. 28*, 34−42.
Wisniewski, T., & Frangione, B. (1992) *Neurosci. Lett. 135*, 235−238.
Wisniewski, T., Castaño, E. M., Golabek, A., Vogel, T., & Frangione, B. (1994) *Am. J. Path. 145*, 1030−1035.
Yankner, B. A., Duffy, L. K., & Kirschner, D. A. (1990) *Science 250*, 279−282.
Yang, F., Mak, K., Vinters, H. V., Frautschy, S. A., & Cole, G. M. (1994) *NeuroReport 5*, 2177−2120.
Younkin, S. G. (1995) *Ann. Neurol. 37*, 287−288.

BI951685W